

Bonding Assembled Colloids without Loss of Colloidal Stability

Hanumantha Rao Vutukuri,* Johan Stiefelhof, Teun Vissers, Arnout Imhof, and Alfons van Blaaderen*

In recent years the diversity of self-assembled colloidal structures has strongly increased, as it is fueled by a wide range of applications in materials science and also in soft condensed-matter physics.^[1–4] Some potential applications include photonic bandgap (PBG) crystals, materials for plasmonic devices, high-efficiency energy conversion and storage, miniature diagnostic systems, desalination, and hierarchically structured catalysts.^[1–4] Three dimensional colloidal crystals with mostly close-packed (randomly or face-centered cubic (fcc) stacked) structures have been fabricated via various methods, some of which are able to impose the orientation of these crystals, e.g., sedimentation,^[5] colloidal epitaxy,^[6] evaporative or “flow controlled” deposition,^[7] shear flow,^[8,9] and spin-coating.^[10] Fewer methods have been reported to generate non-close-packed colloidal crystal structures, for instance, by a physical or chemical immobilization of colloidal arrays with a readily polymerizable monomer, which is dissolved in the dispersion,^[11–14] and by a combination of thermal sintering and etching of close-packed colloidal crystals.^[15] Many methods are currently being developed further to fabricate more diverse crystal symmetries and non-close-packed structures by tuning the interaction between the particles, e.g., oppositely charged interactions,^[16,17] external electric fields,^[18–20] and/or non-spherical shapes.^[21,22] However, the structures thus formed are vulnerable to capillary forces that arise when the solvent is evaporated and to many other post-treatment steps, especially when the particles are non-close-packed.^[1–4] For example, to obtain a PBG in the near infrared, the artificial opals must be dried, then infiltrated with a high-refractive-index material, and the spheres must subsequently be selectively removed by chemical etching^[15,23] or a thermal treatment (calcination or pyrolysis).^[1,2,4,14,24]

Here, we present a facile and flexible one-step, in situ, thermal annealing method to permanently fix non-close-packed and close-packed polymeric structures so that they easily survive a subsequent drying step without loss of colloidal stability. We first demonstrate the concept with fluorescently labeled and sterically stabilized polymethylmethacrylate (PMMA) particles^[25] because this system can be readily index and density matched, allowing

us to compare their structures in 3D real-space before and after the treatment by means of confocal laser scanning microscopy. In unrelated work, we have already demonstrated this method for creating 1D colloidal bead chains by the application of an external electric field,^[26] but it is shown in the present paper that the method presented is quite general and can be applied on many other self-assembly schemes. Moreover, we show that the shape and volume fraction of the particles after bonding can be changed by varying the heating time.

Here, we implement our method to three different non-close-packed assemblies and one close-packed structure: i) ionic colloidal crystals of oppositely charged particles with a CsCl morphology, ii) external electric field induced body-centered tetragonal (bct) crystal structures, iii) labyrinthine or maze-like sheet structures induced by external electric fields, and iv) random hexagonal close-packed crystals.

Recently, it has been demonstrated that cesium-chloride-type (CsCl) crystals can be fabricated from a binary mixture of oppositely charged colloids in a density- and refractive-index-matched low-polar solvent mixture of cyclohexyl bromide (CHB) and cis-decahydronaphthalene (cis-decalin) by tuning the salt concentration.^[17] Here, instead of adding salt to the dispersion to induce opposite charges between the two particle species, we functionalized one of the particle species by incorporating the basic monomer 2-(dimethylamino)ethyl-methacrylate during the synthesis. At sufficiently high volume fractions of the two different colloidal species, they acquired opposite charges after mixing them together. We were able to grow crystals (**Figure 1a**) consisting of oppositely charged particles with diameters of 1.11 μm and 1.05 μm . The CsCl structure consists of an equal number of cesium and chloride ions arranged alternately at the vertices of a body-centered cubic lattice, such that each particle has eight dislike neighbors. The maximum packing fraction for a CsCl crystal can be calculated using $\phi_{\text{CsCl}}(\gamma) = \sqrt{3}\pi(1 + \gamma^3) / (2(1 + \gamma)^3)$, where γ is the size ratio.^[16] For our binary system with a size ratio close to unity ($\gamma = 0.9545$), the corresponding maximum volume fraction is 0.68. Although dense, the packing of the CsCl type structure is below that of the hexagonal close-packed (hcp) and fcc structure, which achieve a packing fraction of 0.74. Because of their non-close-packed nature, we observed that it was not feasible to preserve the CsCl structures simply by letting the solvent evaporate; due to the strong drying forces the regular structure was completely lost even after careful and slow drying for about 6–7 days at room temperature. However, we found that the assembled CsCl-type structures could be made to survive the drying step by first performing a simple thermal annealing method.

H. R. Vutukuri, J. Stiefelhof, Dr. T. Vissers, Dr. A. Imhof,
Prof. A. van Blaaderen
Soft Condensed Matter
Debye Institute for Nanomaterials Science
Utrecht University
Princetonplein 1, 3584 CC, Utrecht, The Netherlands
E-mail: H.R.Vutukuri@uu.nl; A.vanBlaaderen@uu.nl



DOI: 10.1002/adma.201104010

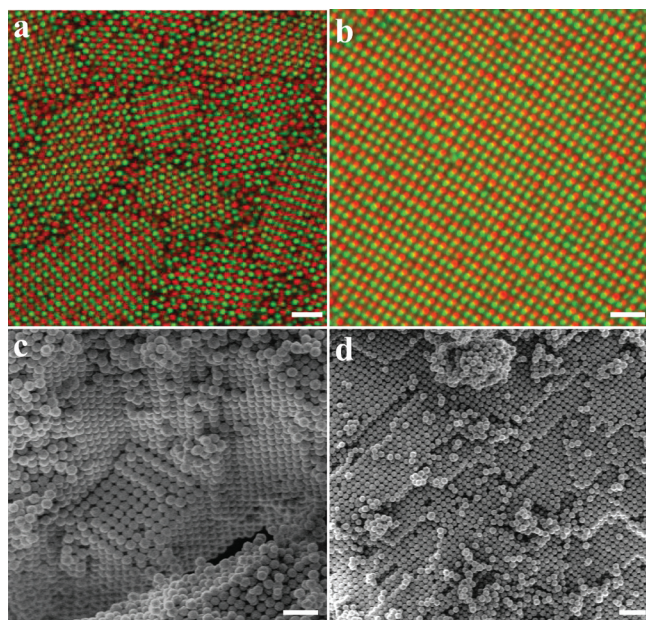


Figure 1. CsCl-type crystals. Confocal 2D $x-y$ microscopy images of positive (red, radius 555 nm) and negative (green, radius 525 nm) PMMA spheres, showing CsCl-like crystals with different orientations, before (a) and after (b) the heat treatment. Note that the images were not recorded at the same spot in the sample. c,d) SEM images of dried CsCl-type crystals showing that the CsCl structure was preserved. Scale bars are 5 μm .

To anneal the crystals, first a CsCl-type crystal was grown in an upright positioned capillary cell of 0.1 mm \times 1.0 mm cross section. The capillary was then immersed in a hot water bath (75 °C) for about 2 min. This was followed by cooling through contact with ambient air. After the heat treatment, all the particles were immobilized and we did not observe any Brownian motion at the single particle level within the structure, which still remained crystalline. Finally, we carefully opened the cell and then dried the crystalline structure for about 6–7 days at room temperature, similar to what was described above for the CsCl crystals that were not first heat treated. Confocal microscopy images of CsCl-type crystals are shown before (Figure 1a) and after (Figure 1b) the heat treatment. Figure 1c,d are scanning electron microscopy (SEM) images of the dried CsCl-type crystals. Clearly the order was well preserved.

To probe the underlying mechanism of bonding between the physically touching neighboring particles we measured the glass transition temperature (T_g) of PMMA particles ($\sigma = 2.30 \mu\text{m}$) in both dry and wet states, as shown in Figure S1 (Supporting Information). The glass transition temperature ($T_g = 144.5^\circ\text{C}$, Supporting Information Figure S1a) of dry PMMA particles was slightly higher than that of the particles in a wet state ($T_g = 142.5^\circ\text{C}$, Supporting Information Figure S1b). Note that the measurement was done 5 min after the sample preparation (42 wt%). The glass transition temperature decreased further ($T_g = 137.8^\circ\text{C}$, Supporting Information Figure S1c) when the sample had been allowed to equilibrate for about 7–8 days. We suspect this effect was the result of a slight swelling of the PMMA particles in cyclohexyl bromide (CHB). Our bonding temperature was 70–75 °C, which is still well below

the glass transition temperature of PMMA particles in both dry and wet states. Therefore it is unlikely that viscous flow took place between the physically touching neighboring particles during the bonding step. We believe that an explanation for the bonding of particles may be found in the fact that at elevated temperatures, the steric poly-12-hydroxystearic acid (PHSA)–PMMA comb-graft stabilizer that is present on the surface of the particles^[25] redistributes so that the particles that are in contact bond (fuse) together permanently by the same van der Waals forces between the PMMA polymers that keep the uncross-linked particles together. Once the dispersion was brought back to room temperature, the steric stabilizer apparently rearranged to its original state because the particle assemblies became stable again, as we will show later. Hence particle stability by steric stabilization was not lost after the bonding.

External electric fields have proven to be a versatile tool to direct colloidal self-assembly into strings (1D),^[26,27] sheets (2D),^[28] and equilibrium 3D crystallites.^[19,20,29,30] Suspensions of particles with long-range screened Coulombic interactions and induced dipolar interactions show especially rich phase behavior.^[20,31] Non-close-packed structures such as body-centred tetragonal (bct) and body-centred orthorhombic (bco) are among the possible crystalline phases for these types of systems. An important feature of the field-induced crystals is their complete crystallinity.

Suspensions consisting of positively charged monodisperse PMMA particles in a nearly refractive-index-matched organic solvent (CHB) were introduced into a thin indium tin oxide coated electric cell.^[18] Large single-domain bct crystallites that do not have a layer of colloidal fluid on top were grown under an external AC field ($E_{\text{rms}} = 0.85 \text{ V } \mu\text{m}^{-1}$, $f = 1 \text{ MHz}$, where E_{rms} is the root-mean-square electric field strength and f is the frequency).^[20] Two things make it difficult to preserve the obtained bct structure during drying: i) the field and solvents that are required for it to exist and ii) it is metastable with respect to a fcc lattice (close-packed) to which it deforms under small perturbations.^[18–20,31] To overcome these limitations, we first immobilized the “wet crystal” using the thermal treatment. The entire sample was heated to 70–75 °C for about 2–3 min using a stream of hot air that was much wider than the sample cell. We kept the field on for 8–10 min more while the sample cell was allowed to cool down to room temperature. The assembled structures remained stable in the liquid even after the electric field was turned off as shown in Figure 2d. Figure 2a,b clearly illustrate the difference between the bct and fcc structures. Figure 2e clearly shows that the bct order was also preserved in the dried form.

For particles interacting as magnetic or dielectric dipoles, labyrinthine patterns can be formed by particles that get stuck in one of the possible local minimum (metastable) energy states rather than being in the ground state as in the case for equilibrium structures.^[18,32,33] The internal structure of the labyrinth is solely dependent on the rate at which the applied field was increased and on initial conditions, which is indicative of a configuration space that has a vast number of local energy minima.^[33,34] However, these labyrinthine structures do slowly evolve to form 3D crystals.^[18,20]

At a moderate particle concentration ($\phi = 0.20$, $\sigma = 2.3 \mu\text{m}$, where ϕ is the volume fraction and σ is the particle diameter)

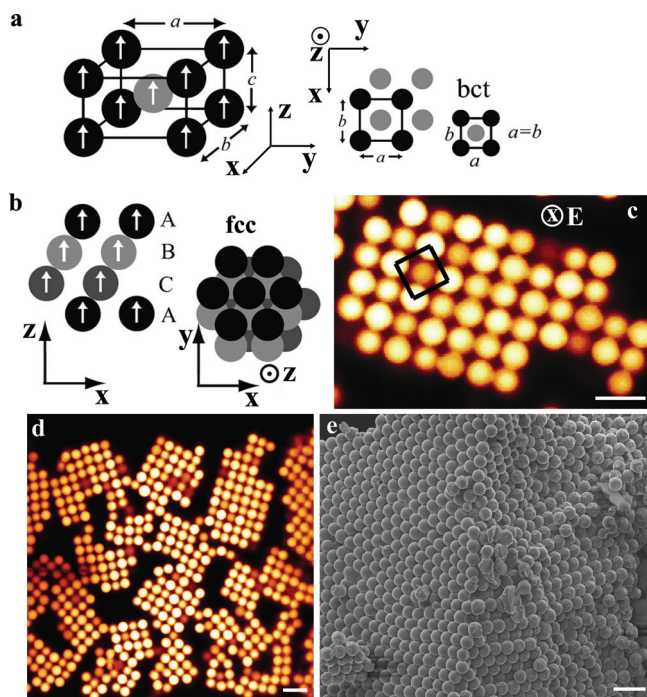


Figure 2. Large permanent bct crystallites were fabricated from 2.1 μm PMMA particles in CHB. a) Unit cell of the bct crystal. The white arrows indicate the direction of the field-induced dipole moments. The bct structure corresponds to $a = b \neq c$. The top-view of the body-centered structure can be constructed by placing strings of particles (with c being the interparticle distance in the strings) shifted by $c/2$ into two interpenetrating rectangular lattices. b) For comparison, the fcc structure is shown in side ($x-z$) and top ($x-y$) views. c) A confocal microscopy image that clearly reveals the characteristic bct stacking: a square arrangement of spheres perpendicular to the applied electric field (the top layer is indicated with the square outline). d) Confocal microscopy image of an $x-y$ slice in the mid-plane of the heat-treated sample in the absence of the applied electric field. e) SEM image of a dried bct structure. Scale bars are 5 μm .

and field strength ($E_{\text{rms}} = 0.70 \text{ V } \mu\text{m}^{-1}$, $f = 1 \text{ MHz}$), a labyrinthine structure was observed when the field was increased from 0 to $0.70 \text{ V } \mu\text{m}^{-1}$ in less than 30–45 s. The labyrinthine structures rely on the presence of an external electric field, i.e., particles disperse again when the field is switched off. After the structure had formed the entire sample was heated to 70–75 $^{\circ}\text{C}$ for about 2–3 min. Upon subsequent removal of the field, a confocal microscopy image (Figure 3a) revealed that the structure was completely preserved. We believe that these structures are interesting model systems to study the diffusion of tracer particles in porous materials^[32] and that they are also useful for the fabrication of materials, which rely on strongly anisotropic arrangements of the particles, such as field-structured composites, for efficient and directed heat transfer.^[35]

Colloidal self-assembly by sedimentation is one of the most common and simple techniques for making colloidal crystals for a range of applications.^[4–6,36] Close-packed structures can be easily preserved simply by controlled drying. Here, we present a new in situ method to permanently preserve the crystalline structure in a more robust way. A large random hexagonal close-packed (rhcp) crystal (Figure 4a) was grown by sedimentation from a nearly refractive-index-matched hard-sphere-like

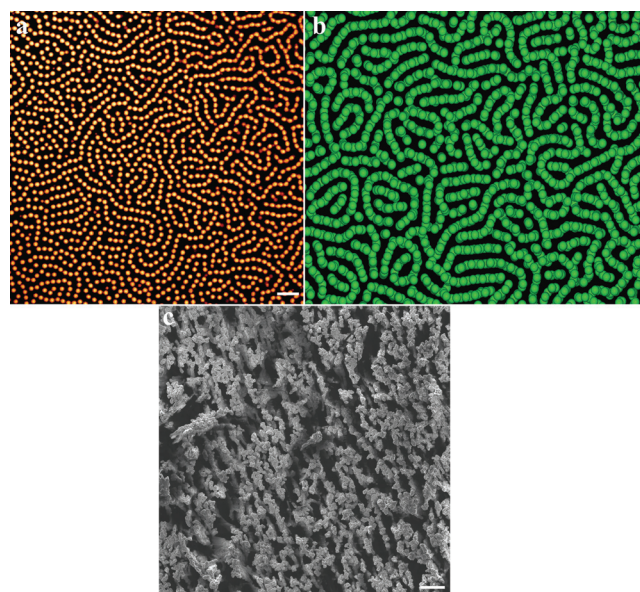


Figure 3. Labyrinth structure consisting of 2D particle sheets oriented in the direction of the applied field (field is perpendicular to the imaging plane) at a packing fraction of about 20%. a) Confocal microscopy image showing a cross section of a permanently bonded labyrinth pattern in the absence of the applied electric field. b) Rendered particle coordinates revealing the 3D network of the permanently bonded structure. c) SEM image of a labyrinth structure that has been immobilized by thermal annealing. Scale bars are 10 μm .

colloidal dispersion (3.1 μm PMMA particles in salt saturated CHB) in a capillary cell of 0.1 mm \times 2.0 mm. The capillary cell was then immersed into a hot water bath at 80 $^{\circ}\text{C}$ for about 2–3 min. Next, the cell was carefully opened and subsequently the crystalline structure was dried for about 6–7 days at room temperature (Figure 4b).

In an identical sample, the close-packed particles were heated for 15–20 min. The surface tension forces^[37,38] between the particles and the solvent caused them to deform from a sphere to a rhombic dodecahedron (Figure 4c). It is well known that even for homogeneous polymer particles the glass transition temperature for the outer layer of the polymer can differ significantly (tens of degrees) from that of the interior.^[39–41] This sintering process has been discussed in the literature using a range of models arising from either a viscous flow process driven by surface tension effects or an elastic Hertzian deformation of elastic spheres under tension. Almost certainly, the reality is some more complex viscoelastic intermediate form where the details depend mostly on particle and stabilizer properties.^[42] By varying the heating time we were able to tune the packing fraction within the crystalline structure, as was shown before for latex film formation^[37,38] and annealed inorganic colloidal crystals of silica particles at elevated temperatures.^[15,43] Moreover, tuning PBG properties in this way could also be possible.^[43,44]

Finally, we heated the sample cell at elevated temperatures (95 $^{\circ}\text{C}$) for a longer period of time, about 2.5–3.0 h. The space-filling rhombic dodecahedron structures (Figure 4c) then transformed into thin films by polymer interdiffusion across the boundaries (Figure 4d). This interdiffusion process is also expected to increase the mechanical strength of the polymer film.^[45]

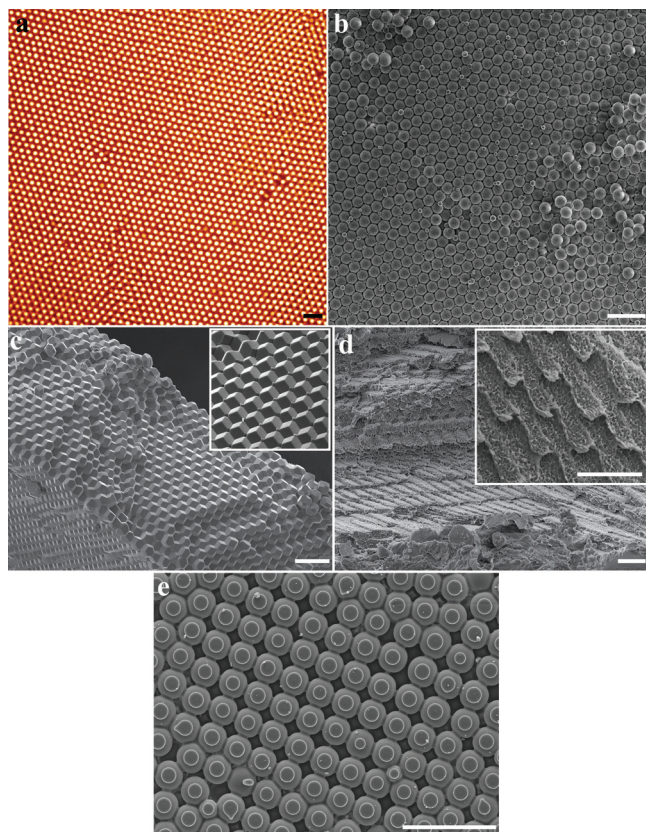


Figure 4. Close-packed hard-sphere crystal. a) Confocal microscopy image of the rhcp crystalline structure. b–d) SEM images of dried hard-sphere crystals that were annealed at different temperatures (T) and heating times (t_h): b) $T = 70\text{ }^{\circ}\text{C}$ and $t_h = 2\text{--}3\text{ min}$, c) $T = 80\text{ }^{\circ}\text{C}$ and $t_h = 15\text{--}20\text{ min}$, and d) $T = 95\text{ }^{\circ}\text{C}$ and $t_h = 2.5\text{--}3\text{ h}$. In panels (c,d) the upper inset shows a magnified view of the internal structure. e) SEM image of a bct crystal that shows the square arrangement of spheres perpendicular to the applied field. Note that the particles that were in contact with each other had bonded permanently. A small portion of the spheres in the first layer were flattened by the electrode wall. Scale bars are $10\text{ }\mu\text{m}$.

Moreover, our method can easily be extended to different self-assemblies of particles. For example, Figure 4e illustrates the start of particle deformation in films of bct crystals that assembled in an electric field. The SEM image shows particles that are touching an electrode.

An interesting feature of our method is that the permanently bonded and dried structures could be used either as seeds for crystal nucleation and growth studies^[6,46,47] or for a successive self-assembly process. Additionally, the permanently bonded structures can readily be redispersed and remain stable afterwards (see Supporting Information).

In summary, we have demonstrated a simple and efficient thermal annealing method to bond colloids together permanently after an initial self-assembly step without loss of colloidal stability. Subsequently, these structures can be used in a second self assembly step and/or in further processing steps such as drying and chemical depositions.^[1,2,4,23,24] We strongly believe that our method will work with many (sterically stabilized) polymer colloids and could also be easily extended to

more complex core/shell architectures in case the outer layer is a polymer layer.

Experimental Section

PMMA particles were synthesized by dispersion polymerization, covalently labeled with the fluorescent dye 7-nitrobenzo-2-oxa-1,3-diazol (NBD) or rhodamine isothiocyanate (RITC), and sterically stabilized with poly(12-hydroxystearic acid).^[25] $1.05\text{ }\mu\text{m}$, $1.10\text{ }\mu\text{m}$, $2.05\text{ }\mu\text{m}$, $2.35\text{ }\mu\text{m}$, and $3.10\text{ }\mu\text{m}$ PMMA spheres in nearly density-matched mixtures of the low-polar solvents CHB and cis-decahydronaphthalene were used. To achieve hard-sphere-like interactions, the 2.05 , 2.30 , 2.35 , and $3.10\text{ }\mu\text{m}$ PMMA particles were dispersed into salt (tetrabutylammonium bromide, TBAB, Sigma) saturated CHB.^[20,28] All solvents were used as received without any further purification. Two types of electric cells were used: rectangular capillaries (VetroCom, UK) and homemade sandwich ITO-coated glass cells. The rectangular sample cells consisted of a $0.1\text{ mm} \times 1.0\text{ mm}$ cross section capillary with two $50\text{-}\mu\text{m}$ -thick nickel-alloy wires (Goodfellow) threaded along the side walls. After the cell was filled with the colloidal suspension, it was sealed with UV-curing optical adhesive (Norland no.68) and the particle dynamics were studied by means of confocal laser scanning microscopy (Leica TCS SP2). A function generator (Agilent, Model 3312 OA) and a wide-band voltage amplifier (Krohn-Hite, Model 7602M) were used to generate the electric fields. After drying the sample, structures that were made permanent by thermal annealing were imaged using SEM (FEI, XL30FEG). Differential scanning calorimetry (HP DSC827e, Mettler-Toledo, USA) was used to measure the glass transition temperature in both dry and wet states.

Acknowledgements

The authors thank J. D. Meeldijk for SEM measurements and Rien van Zwienen and Arjen van de Glind for DSC measurements. This work is part of the research program of the “Stichting voor Fundamenteel Onderzoek der Materie (FOM)”, which is financially supported by the Nederlandse organisatie voor Wetenschappelijke Onderzoek (NWO) within the DFG/FOM program SFB-TR6. H.R.V., J.S., and T.V. were supported by NWO-Chemische Wetenschappen and the EU project (Nanodirect, CP-FP-213948-2).

Received: October 18, 2011

Published online: December 12, 2011

- [1] F. Li, D. P. Josephson, A. Stein, *Angew. Chem. Int. Ed.* **2011**, *50*, 360.
- [2] J. F. Galisteo-López, M. Ibisate, R. Sapienza, L. S. Froufe-Pérez, Á. Blanco, C. López, *Adv. Mater.* **2011**, *23*, 30.
- [3] S. C. Glotzer, M. J. Solomon, *Nat. Mater.* **2007**, *6*, 557.
- [4] A. Stein, F. Li, N. R. Denny, *Chem. Mater.* **2008**, *20*, 649.
- [5] K. E. Davis, W. B. Russel, W. J. Glantschnig, *Science* **1989**, *245*, 507.
- [6] A. van Blaaderen, R. Ruel, P. Wiltzius, *Nature* **1997**, *385*, 321.
- [7] P. Jiang, J. F. Bertone, K. S. Hwang, V. L. Colvin, *Chem. Mater.* **1999**, *11*, 2132.
- [8] A. Imhof, A. van Blaaderen, J. K. G. Dhont, *Langmuir* **1994**, *10*, 3477.
- [9] B. J. Ackerson, P. N. Pusey, *Phys. Rev. Lett.* **1988**, *61*, 1033.
- [10] P. Jiang, M. J. McFarland, *J. Am. Chem. Soc.* **2004**, *126*, 13778.
- [11] J. J. Bohn, M. Ben-Moshe, A. Tikhonov, D. Qu, D. N. Lamont, S. A. Asher, *J. Colloid Interface Sci.* **2010**, *344*, 298.
- [12] S. A. Asher, K. W. Kimble, J. P. Walker, *Chem. Mater.* **2008**, *20*, 7501.
- [13] L. Liu, P. S. Li, S. A. Asher, *Nature* **1999**, *397*, 141.
- [14] J. H. Holtz, S. A. Asher, *Nature* **1997**, *389*, 829.
- [15] R. Fenollosa, F. Meseguer, *Adv. Mater.* **2003**, *15*, 1282.

- [16] P. Bartlett, A. I. Campbell, *Phys. Rev. Lett.* **2005**, 95, 128302.
- [17] M. E. Leunissen, C. G. Christova, A. P. Hynninen, C. P. Royall, A. I. Campbell, A. Imhof, M. Dijkstra, R. van Roij, A. van Blaaderen, *Nature* **2005**, 437, 235.
- [18] U. Dassanayake, S. Fraden, A. van Blaaderen, *J. Chem. Phys.* **2000**, 112, 3851.
- [19] A. Yethiraj, J. H. J. Thijssen, A. Wouterse, A. van Blaaderen, *Adv. Mater.* **2004**, 16, 596.
- [20] A. Yethiraj, A. van Blaaderen, *Nature* **2003**, 421, 513.
- [21] A. Kuijk, A. van Blaaderen, A. Imhof, *J. Am. Chem. Soc.* **2011**, 133, 2346.
- [22] M. Mittal, E. M. Furst, *Adv. Funct. Mater.* **2009**, 19, 3271.
- [23] J. E. G. J. Wijnhoven, W. L. Vos, *Science* **1998**, 281, 802.
- [24] C. I. Aguirre, E. Reguera, A. Stein, *Adv. Funct. Mater.* **2010**, 20, 2565.
- [25] G. Bosma, C. Pathmanoharan, E. H. A. de Hoog, W. K. Kegel, A. van Blaaderen, H. N. W. Lekkerkerker, *J. Colloid Interface Sci.* **2002**, 245, 292.
- [26] H. R. Vutukuri, A. F. Demirörs, B. Peng, P. D. J. van Oostrum, A. Imhof, A. van Blaaderen, unpublished.
- [27] K. D. Hermanson, S. O. Lumsdon, J. P. Williams, E. W. Kaler, O. D. Velev, *Science* **2001**, 294, 1082.
- [28] M. E. Leunissen, H. R. Vutukuri, A. van Blaaderen, *Adv. Mater.* **2009**, 21, 3116.
- [29] T. C. Halsey, W. Toor, *Phys. Rev. Lett.* **1990**, 65, 2820.
- [30] R. C. Hayward, D. A. Saville, I. A. Aksay, *Nature* **2000**, 404, 56.
- [31] A. P. Hynninen, M. Dijkstra, *Phys. Rev. Lett.* **2005**, 94, 138303.
- [32] H. A. Makse, J. S. Andrade, S. H. Eugene Stanley, *Phys. Rev. E* **2000**, 61, 583.
- [33] R. E. Rosensweig, M. Zahn, R. Shumovich, *J. Magn. Magn. Mater.* **1983**, 39, 127.
- [34] A. J. Dickstein, S. Erramilli, R. E. Goldstein, D. P. Jackson, S. A. Langer, *Science* **1993**, 261, 1012.
- [35] J. E. Martin, G. Gulley, *J. Appl. Phys.* **2009**, 106, 084301.
- [36] P. N. Pusey, W. van Megen, *Nature* **1986**, 320, 340.
- [37] A. F. Routh, W. B. Russel, *Ind. Eng. Chem. Res.* **2001**, 40, 4302.
- [38] S. Mazur, R. Beckerbauer, J. Buckholz, *Langmuir* **1997**, 13, 4287.
- [39] O. K. C. Tsui, Z. H. Yang, Y. Fujii, F. K. Lee, C. H. Lam, *Science* **2010**, 328, 1676.
- [40] J. L. Keddie, R. A. L. Jones, R. A. Cory, *Faraday Discuss.* **1994**, 98, 219.
- [41] J. A. Forrest, K. Dalnoki-Veress, J. R. Stevens, J. R. Dutcher, *Phys. Rev. Lett.* **1996**, 77, 2002.
- [42] W. B. Russel, A. F. Routh, *Langmuir* **1999**, 15, 7762.
- [43] H. Miguez, F. Meseguer, C. Lopez, A. Blanco, J. S. Moya, J. Requena, A. Mifsud, V. Fornes, *Adv. Mater.* **1998**, 10, 480.
- [44] B. Gates, S. H. Park, Y. N. Xia, *Adv. Mater.* **2000**, 12, 653.
- [45] S. Prager, M. Tirrell, *J. Chem. Phys.* **1981**, 75, 5194.
- [46] V. W. A. de Villeneuve, R. P. A. Dullens, D. G. A. L. Aarts, E. Groeneveld, J. H. Scherff, W. K. Kegel, H. N. W. Lekkerkerker, *Science* **2005**, 309, 1231.
- [47] A. Cacciuto, S. Auer, D. Frenkel, *Nature* **2004**, 428, 404.